Paper reference: ECF 13 008 04371 X

EFFECTS OF GEOMETRY AND MATERIAL ON THE ENERGY DISSIPATION RATE

W. Brocks[1] and Th. Siegmund[2]

[1)] GKSS Research Centre, Geesthacht, Germany
[2)] Purdue University, West Lafayette, USA

ABSTRACT

The concept of energy dissipation rate toghether with a numerical model which allows for splitting into global plastic work and local work of separation is applied to different specimens and materials, which reveal an extremely different resistance behaviour against ductile crack growth, namely side-grooved C(T) and M(T) specimens of a ferritic steel and thin centre cracked panels with varying crack lengths of an aluminium alloy. In both cases, however, it could be shown, that the dissipated work is mainly due to global plastic deformation of the specimens, once again proving that J_R-curves are not an appropriate measure of a material's fracture toughness. Though the dissipation rate is also geometry dependent, of course, scaling by limit load factors of the respective geometries is succesful in certain cases which opens perspectives for transfering experimental data from one geometry to another. The applied cohesive zone model is not only an effecitive tool for simulating crack growth phenomena but provides a method of characterizing the materials resistance against ductile crack extension by two parameters, namely the cohesive strength, σ_{max}, and the separation energy, Γ_c,

INTRODUCTION

The concept of energy dissipation rate, $R = dU_{dis}/da$, as proposed by TURNER [1] has brought some better understanding of ductile tearing resistance. The rate quantity R, which measures the increment of irreversible external work necessary to propagate the crack by some amount, Δa, is physically more meaningful for describing the resistance of a structure against ductile crack extension than the conventionally used cumulative J integral. Whereas J_R-curves keep rising even for steady state crack extension, R was shown to decrease with Δa and approach a stationary value [2].

Nevertheless, the new concept has not yet found wide acceptance in application, since R, like J, depends on the geometry and the type of loading of the specimen or the structure. Hence, it does not solve the problem of missing transferability of resistance curves. It has been shown for a ferritic steel and two specimen types, namely a C(T) and a M(T) specimen, that this geometry dependence could be scaled by their respective limit load factors [3]. However, a detailed study on the geometry effects on $R(\Delta a)$ curves for various materials and specimen geometries [4] exhibited limitations of this scaling.

Classical elastic-plastic fracture mechanics suffers from the inherent inability of separating local work of fracture from global work of (remote) plastic deformation. Numerical simulations however make it possible to split up the total dissipated energy [5], within the limitations of any model, of course. This is illustrated on numerical simulations of experimental tests.

DEFINITION AND EVALUATION OF *R*

Since GRIFFITH's considerations on rupture in solids the "energy approach" to fracture phenomena has become one of two supporting legs of fracture mechanics. It is based on the material independent law of conservation of energy which under quasistatic conditions, is written down for an incremental process between times t and $t+\Delta t$ involving a crack extension of area $\Delta A = \dot{A}\Delta t$ as

$$\dot{W}_{ex} = \dot{U}_{el} + \dot{U}_{pl} + \dot{U}_{sep}, \tag{1}$$

where W_{ex} is the work done by external forces, U_{el} and U_{pl} are the elastic and plastic part of the deformation energy, and U_{sep} is the "work of separation" in the process zone which is necessary to create new surfaces. The principal difficulty in elastic-plastic fracture mechanics consists in separation of the two dissipative terms in the balance of power, namely the rates of plastic work and fracture energy. Such seperation would be necessary in order to formulate a relevant fracture criterion, since U_{pl} is not a material constant but depends on geometry and loading conditions. In the R-curve method, the difference between the two terms is not recognized leading to a number of inconsistencies well known as "constraint effects".

KOLEDNIK [6] gave obvious examples what J-Δa curves really mean in gross plasticity. Many attempts have been made to split the dissipated energy into (local) fracture energy and (global) plastic energy, but did not yet yield satisfactory results. TURNER [1] doubted that splitting dissipation into fracture and plasticity is possible at all and suggested the combined plastic plus fracture dissipation rate

$$R = \frac{dU_{dis}}{dA} = \frac{dU_{pl}}{dA} + \frac{dU_{sep}}{dA} = \frac{d\left(W_{ex} - U_{el}\right)}{dA} \tag{2}$$

to be fundamental to plastic tearing.

However, BARENBLATT's 40 years old idea [7] of a cohesive zone at the crack tip is the key to a model which allows for splitting the total dissipated energy into local and global contributions [4]. Its application has suffered from the fact that the traction-separation law, σ_n - δ_n, within the cohesive zone cannot be determined experimentally. The increasing potential of numerical simulations has opened a possibility of determining the parameters of a postulated relation from experimental data by an inverse method.The present study adopts a formulation of NEEDLEMAN [8]

$$\sigma_n = \sigma_{max}\, e\, z \frac{\delta_n}{\delta_c} \exp\left(-z\frac{\delta_n}{\delta_c}\right), \tag{3}$$

where e = exp (1) and z = 16 e / 9. Eqn 3 involves two material parameters, the cohesive strength, σ_{max}, and the cohesive length, δ_c, or alternatively the separation energy, Γ_c,

$$\Gamma_c = \frac{9}{16}\sigma_{max}\delta_c. \tag{4}$$

The two contributions to the dissipation rate, Eqn. 2, can be calculated within a finite element analysis as

$$\dot{U}_{pl} = \int_V \sigma_e \dot{\varepsilon}_{pl}\, dV \qquad \text{and} \qquad \dot{U}_{sep} = \int_{\delta_n=0}^{\delta_c} \sigma_n\, d\delta_n \dot{A} = \Gamma_c \dot{A}, \tag{6}$$

respectively, assuming that material damage and final separation occurs in the cohesive zone, only, which is embedded in an elastic-plastic continuums, see Figure 1. The cohesive zone is modelled by special user defined elements in the FE code ABAQUS.

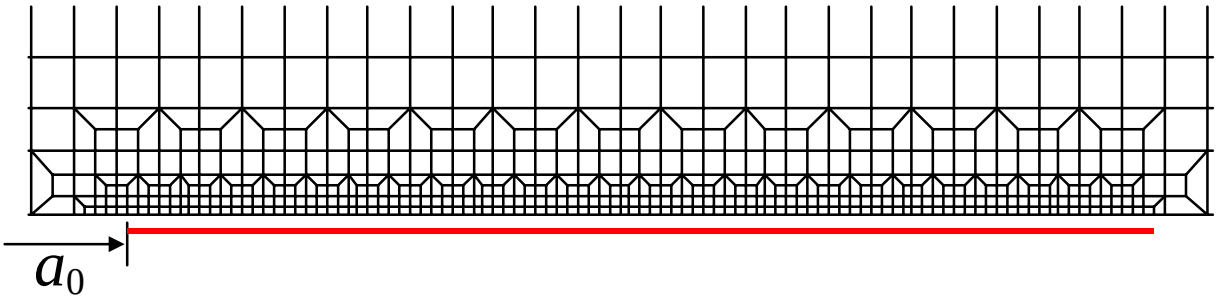

Figure 1: Finite element mesh with cohesive elements in the ligament

RESULTS

The above model was applied to simulate crack growth in

- a side-grooved M(T), $2W$ = 100 mm, a_0/W = 0.49, and a side-grooved C(T) specimen, W = 50 mm, a_0/W = 0.59, respectively, of StE 460, both under conditions of plane strain, see [9, 10], and
- thin centre cracked panels, $2W$ = 508 mm, B = 1.0 mm, a_0/W = 0.2, 0.35, 0.55, of Al 2024 T3, under condition of plane stress, see [11].

All the simulations are based on experimental tests [12, 13]. Ductile crack initiation occurred under fully plastic conditions in the ferritic steel, and under contained yielding in the aluminium sheets. The cohesive parameters used for the numerical simulations were

- σ_{max} = 3.36 σ_Y = 1579 MPa and Γ_c = 53.3 N/mm for the side-grooved steel specimens, and
- σ_{max} = 2 σ_Y = 570 MPa and Γ_c = 17 N/mm for the thin aluminum sheets.

As has been shown in [9], these parameters will depend on the stress triaxiality, in general, which especially becomes evident from the σ_{max} values for the plane strain and the plane stress case, respectively.

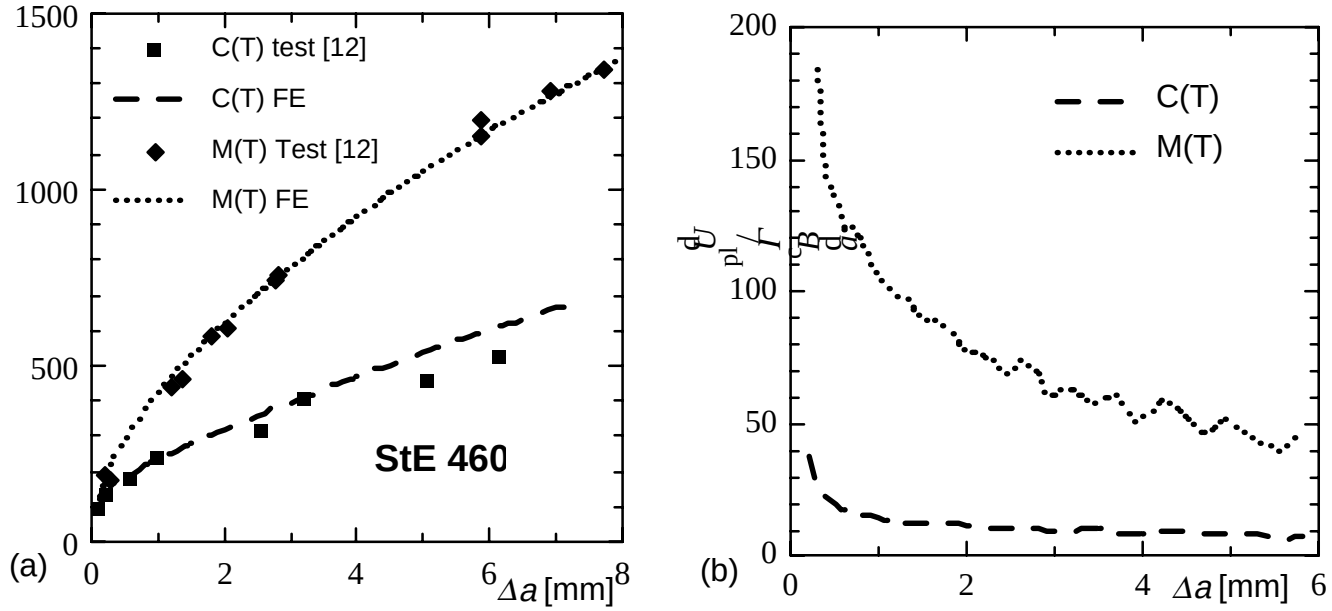

Figure 2: C(T) and M(T) specimens of StE 460,
(a) J_R-curves from fracture tests and numerical simulations,
(b) rate of plastic work normalized by work of separation

Figure 2a shows a comparison of test results [12] with numerical simulations [10] for the M(T) and the C(T) specimen of StE 460 confirming the good performance of the model. The numerically calculated global plastic work per crack increment is shown in Figure 2b. It decreases with crack growth and approaches a stationary value which is around five times higher for the M(T) than for the C(T). And it is by a factor of 10 to 30 for the C(T) and 50 to 150 for the M(T) greater than the local work of separation, which means that for the ferritic steel "fracture resistance", as measured by an R-curve test, is mainly due to global plastic deformation of the specimen or structure. This is confirmed by Figure 3a where a plastic J value is calculated from the accumulated plastic work by

$$J_{\mathrm{pl}} \approx \frac{\eta}{W-a_0}\int_0^{\Delta a}\frac{dU_{\mathrm{pl}}}{da}da + J_i \quad \text{with} \quad \eta = \begin{cases} 2.26 \text{ for C(T)} \\ 1.0 \quad \text{for M(T)} \end{cases} \tag{7}$$

and compared to the experimental (total) J. This explains the geometry dependence of J_{R}-curves as well as the scaling properties of the limit load factor,

$$R_n = \sigma_Y (W-a_0)\frac{\sigma_Y}{E}\cdot f_Y \tag{8}$$

with
$$f_Y = \begin{cases} \dfrac{2}{\sqrt{3}}\cdot\dfrac{-\left(1+1.702\,\dfrac{a_0}{W}\right)+\left[2.702+4.599\left(\dfrac{a_0}{W}\right)^2\right]^{1/2}}{1-\dfrac{a_0}{W}} & \text{for C(T)} \\ \dfrac{2}{\sqrt{3}} & \text{for M(T)} \end{cases}, \tag{9}$$

see [13] and Figure 3b, where the rate of plastic work is normalized by R_{n}, bringing the curves of C(T) and M(T) together and thus render transferability.

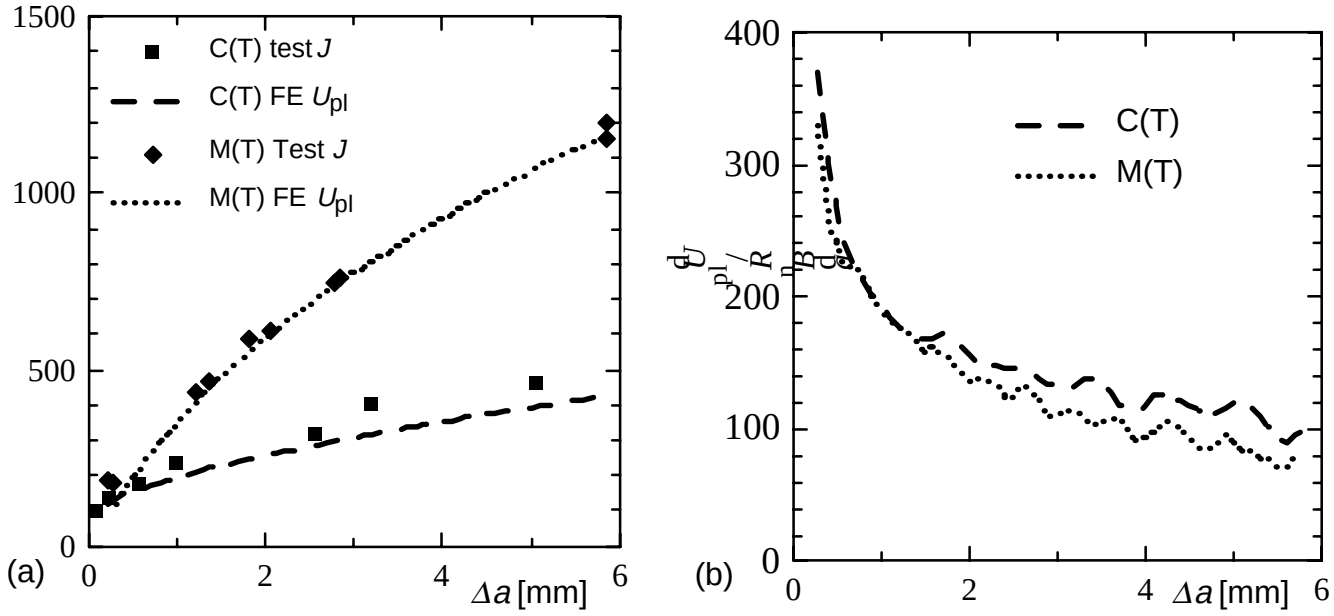

Figure 3: C(T) and M(T) specimens of StE 460,
(a) J_{R}-curves from tests and from accumulated plastic work Eqn 7,
(b) rate of plastic work normalized by limit load factor Eqn 3.

Figure 4a displays a comparison of test results [13] with numerical simulations [11] for the thin aluminium centre cracked panels. The numerically calculated dissipated work, i.e. work of global plastic deformation plus local separation, is plotted in Figure 2b increasing almost linearly with crack growth and depending on the initial crack lengths, of course.

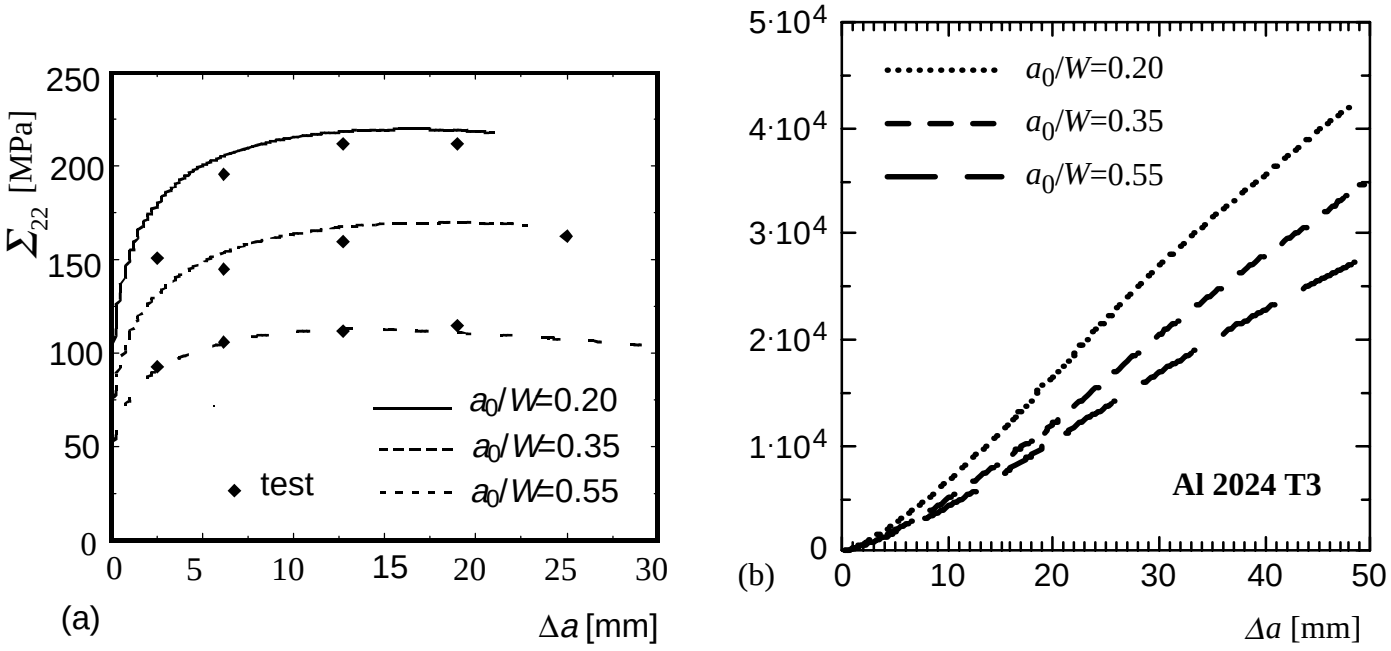

Figure 4: Centre cracked panels of Al 2024 T3,
(a) tests and numerical results of applied stress vs crack growth,
(b) accumulated plastic work from FE simulation.

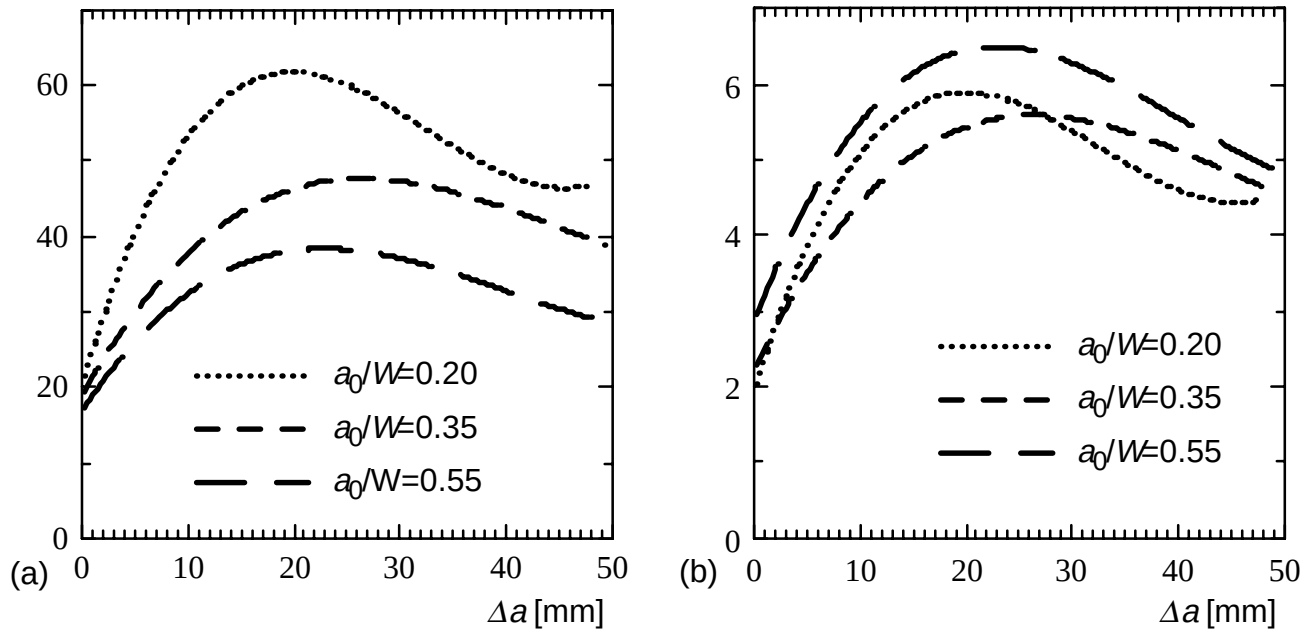

Figure 5: Centre cracked panels of Al 2024 T3,
(a) rate of plastic work normalized by work of separation,
(b) rate of plastic work normalized by limit load factor Eqn 3.

As ductile crack initiation occurs under contained yielding the dependence of the dissipation rate on crack extension looks much different, see Figure 5a, from that for the ferritic steel, see Figure 2b. It does not decrease monotonically as in Figure 3b but displays a maximum after 20 to 30 mm of crack growth which

corresponds approximately to the load maximum in Fig 4a and presumably with reaching a fully yielded condition. Normalization by the local work of separation, Γ_c, shows again that a great part of the dissipated work is due to plastic deformation as R is 20 to 60 times higher than Γ_c,, see Figure 5a. Normalization by the plastic limit load factor of Eqn 3 with $f_Y = 1$ for plane stress has some scaling effect on the dissipation rates for the three crack lengths and brings the three curves closer together, see Figure 5b.

CONCLUSIONS

The dissipation rate, R, characterizes the resistance of a structure against ductile crack propagation. It is, hence, geometry dependent, as it includes the total work of plastic deformation per crack increment. Numerical modelling helps to overcome the fundamental deficiency of classical elastic-plastic fracture mechanics, i.e. its inability of separating local work of fracture from work of remote plasticity. This splitting is realized by introducing a cohesive zone in the crack ligament where material separation is supposed to be localized. The model was successfully applied to various materials and specimens which had been chosen since they show an extremely different crack resistance behaviour.
It was found that

- a great part of the dissipated work is due to global plastic deformation, explaning the geometry dependence of J_R-curves which represent accumulated dissipated work,
- normalization of R-Δa-curves by a plastic limit load factor has some scaling effect with respect to a geometry independent description of crack growth resistance.

The applied cohesive zone model is not only an effecitive tool for simulating crack growth phenomena but provides a method of characterizing the materials resistance against ductile crack extension by two parameters, namely the cohesive strength, σ_{max}, and the separation energy, Γ_c,

REFERENCES

1. Turner, C.E. (1990) in: *Fracture Behaviour and Design of Materials and Structures, Proc. ECF 8,* pp. 933-949, Firrao, D. (Edt), Engineering Mechanics Advisory Services (EMAS), Warley (UK).
2. Memhard, D., Brocks, W., and Fricke, S. (1993), *Fatigue Fract. of Engng. Mater. Struct.* **16**, pp. 1109-1124.
3. Memhard D., Brocks, W., and Fricke, S. (1994) in: *Structural Integrity - Experiments, Models, Applications Proc. ECF 10*, pp. 149-158, Schwalbe, K.-H. und Berger, Ch. (Eds), Engineering Material Advisory Services (EMAS), Warley (UK).
4. Brocks, W. (1998) *Technical Note GKSS/WMG/98/6*, GKSS Research Centre Geesthacht.
5. Siegmund, Th., and Brocks, W. (1999), *Int. J. Fracture* **99**, pp. 97-116.
6. Kolednik, O. (1991), *Engineering Fracture Mechanics* **38**, pp. 403-412.
7. Barenblatt, G.I. (1962), *Advances in Applied Mechanics* **7**, pp.55-129.
8. Needleman, A. (1990), *Int. J. Fracture* **42**, pp.21-40.
9. Siegmund, Th., and Brocks, W. (2000), *Fatigue and Fracture Mechanics: 30th Volume, ASTM STP 1360*, pp. 139-151, Paris, P.C. and Jerina, K.L. (Eds), American Society for Testing and Materials.
10. Siegmund, Th., Bernauer,G., and Brocks, W. (1998) in: *Fracture from Defects, Proc. ECF 12*, Vol. II, pp. 933-938, Brown, M.W., de los Rios, E.R., Miller, K.J. (Eds), Engineering Materials Advisory Services (EMAS), Warley (UK).
11. Siegmund, Th., and Brocks, W. (2000), *Fatigue and Fracture Mechanics: 31st Volume, ASTM STP 1389*, Halford, G.R. and Gallagher, J.P. (Eds), American Society for Testing and Materials, in press.
12. Häcker, R., Gerwien, P., Thiemich, K.-D., Wossidlo, P., and Baer, W. (1993), *Report BAM-1.31 93/3*, Federal Institute of Material Testing, Berlin.
13. Broek, D., Thomson, D., and Jeong, D.Y. (1994) in: *FAA-NASA Int. Symp. Advanced Structural Integrity Methods for Airframe Durability and Damage Tolerance, NASA Conf. Publ. 3272*, Part II, pp. 85-98.